Theory of frequency-modulation spectroscopy of coherent dark resonances

Julia Vladimirova, Boris Grishanin, Victor Zadkov, Valerio Biancalana†, Giuseppe Bevilacqua†, Evelina Breschi†, Yordanka Dancheva†, and Luigi Moi†

International Laser Center and Faculty of Physics, M. V. Lomonosov Moscow State University, Moscow, Russia

†Department of Physics, University of Siena, via Banchi di Sotto 55, 53100 Siena, Italy

ABSTRACT

Theoretical model for the frequency-modulation spectroscopy of dark resonances is discussed in detail on example of a three-level quantum system in Λ-configuration driven by resonant laser field(s) with and without frequency modulation using two simulation techniques—the density matrix and quantum trajectories analysis.

Keywords: frequency modulation spectroscopy, dark resonances

1. INTRODUCTION

The coherent population trapping (CPT) phenomenon is currently widely used in different applications such as magnetometry, metrology, and others [1–6]. It is most conspicuous for the Λ-transition between two closely spaced long lived levels optically coupled to a third distant short lived level by two continuous coherent radiation fields (Fig. 1). In absorption spectra, coherent superposition of closely spaced levels leads to a very narrow dip of induced transparency or, equivalently, to a non-absorbing dark resonance when resonance fluorescence is observed.

The basics of CPT phenomenon are well understood in the frame of three-level analytical model [7]. For the case of multilevel systems, however, the simple model has to be significantly complicated and analytical results in most cases became impossible [8]. Enriched energetic structure of multilevel atoms, especially in the presence of an external magnetic field, also results in essential modification of the resonance dependencies on driving fields parameters.

Despite the conventional experimental technique for observing the dark resonances spectra with the use of two resonant laser fields described above is now widely used for many applications, still there is a need in elaborating simpler experimental techniques, which would, for instance, employ only one laser field, but with frequency modulation (FM), which also allow the spectroscopy of dark resonances in multilevel atoms. Such experiments are conducted by the group of Prof. Luigi Moi at the University of Siena in Italy [9] and they, in fact, initiated the current theoretical study of interaction between the three-level system in Λ-configuration with the frequency-modulated laser field.

In a typical experiment on FM-spectroscopy of coherent dark resonances of Cs atoms, the atomic media is placed in a homogeneous magnetic field, whose value is in the range of few 10 μT. The coherent resonance is observed when the laser emission, which is frequency modulated, contains in its spectrum a number of frequency components that are in resonance with the atomic levels, i.e., the frequency difference between these components matches the Zeeman splitting ω_{12} of the ground-state sublevels (Fig. 1) due to the presence of dc magnetic field. The laser spectrum is tailored via diode laser frequency modulation obtained by direct modulation of the laser junction current. The coherent structure can be then seen scanning the modulation frequency in a small range around the two-photon resonance condition, or at a fixed modulation frequency scanning the magnetic field in the corresponding range [9–12].

Despite obvious simplicity of this method, analysis of the spectrum becomes a separate problem as a theoretical model for the FM-spectroscopy of dark resonances does not exist to our knowledge so far.

E-mail: vyulia@comsim1.phys.msu.su

ICONO 2005: Nonlinear Laser Spectroscopy, High Precision Measurements, and Laser Biomedicine and Chemistry, edited by Sergey Bagayev et al., Proc. of SPIE Vol. 6257, 625704, (2006)
0277-786X/06/$15 · doi: 10.1117/12.677920

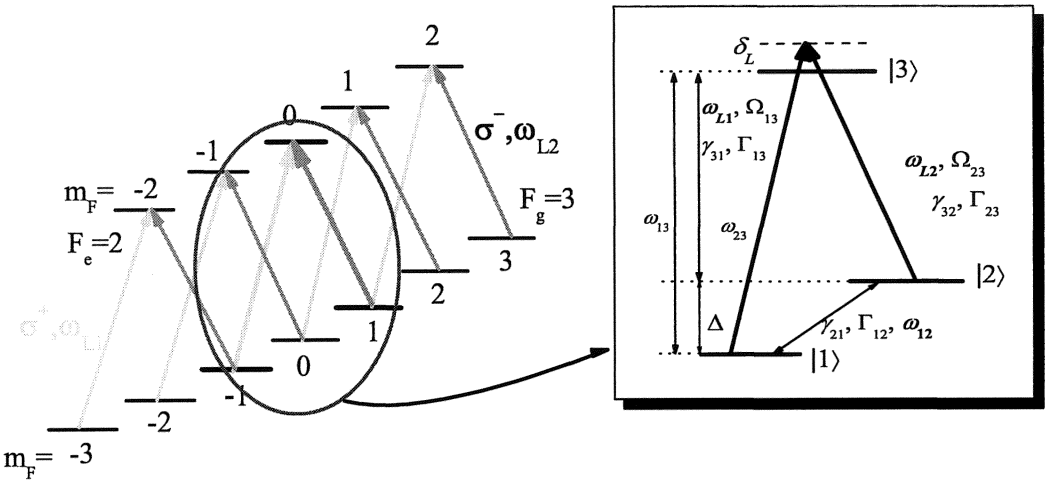

Figure 1. Λ systems formed of the Zeeman sublevels in the $F_g = 3 \rightarrow F_e = 2$ transitions excited by the σ^+ and σ^- components of the respective frequencies ω_1 and ω_2, whose difference is equal to the splitting of the Zeeman sublevels with $\Delta m_F = 2$. Three-level system in Λ-configuration has the following parameters: ω_{L1}, ω_{L2} are the frequencies of the laser fields driving transitions of the system; Ω_{13}, Ω_{23} are the respective Rabi frequencies; δ_L is the frequency detuning from the $|1\rangle \leftrightarrow |3\rangle$ transition; γ_{31}, γ_{32} are the decay rates from excited state $|3\rangle$ onto the low-laying levels $|1\rangle$ and $|2\rangle$; γ_{12} and w are the decay and pumping rates of the level $|1\rangle$ via the level $|2\rangle$, correspondingly; Γ_{31}, Γ_{32}, and Γ_{12} are the dephasing rates for the transitions $|1\rangle \leftrightarrow |3\rangle$ and $|2\rangle \leftrightarrow |3\rangle$, and $|1\rangle \leftrightarrow |2\rangle$, respectively.

In this paper, we present a detailed study of the dynamics of a three-level quantum system in Λ-configuration driven by resonant laser field(s) with and without frequency modulation using two simulation techniques—the density matrix and quantum trajectories analysis.

The paper is organized as follows. General theoretical background for both density matrix and quantum trajectories analysis used for numerical simulation of the fluorescence spectrum of the driven Λ-system is given in Sec. 2. In Sec. 3 we consider physical quantities that are of interest and can be measured experimentally. They include the total fluorescence intensity in equilibrium and in the transient response, resonance fluorescence spectrum, linear and nonlinear absorption coefficients, and the refractive indices. In Sec. 4 two considered above computer simulation techniques are applied for the analysis of a driven Λ-system in both cases, when the frequency modulation is switched off (Sec. 4.1) and on (Sec. 4.2), respectively. Calculations are made for the fluorescence intensity. Finally, the conclusions are summarized in Sec. 5.

2. THEORETICAL ANALYSIS OF TEMPORAL DYNAMICS OF A DRIVEN Λ-SYSTEM

Theoretical analysis of a driven Λ-system can be done both analytically and with the help of various computer simulation techniques. Analytical approach that can be developed, for instance, with the help of diffusion approximation of atomic system under broadband excitation, have obviously rather limited application just to the simplest case of a model three-level atom and cannot be easily extended onto the case of multilevel atoms in an external magnetic field (for example, Cs or Rb atoms) which are of practical interest. It will be discussed elsewhere in a separate publication.

In this section, we will focus on the numerical simulation techniques, which can adequately be used for simulating fluorescence spectrum of both a model Λ-system and a multilevel atom driven by the frequency-modulated laser field(s). With these notes in mind, there exist two key computer simulation techniques suitable for our purpose, namely, the technique based on the solving the master equations for the density matrix (we will call it the *density matrix analysis*) and quantum trajectories technique (we will call it the *quantum trajectories analysis*) [13–16].

Note that the results of the density matrix and quantum trajectories analysis have to be identical within a certain error, which depends on how many trajectories we calculated and averaged over and how precisely we solved master equation and for how long time.

In application to the analysis of multilevel atomic systems, the key difference between these two techniques is as follows. The density matrix technique is used primarily for analysis of atomic systems with rather limited number N of energy levels because the number N^2 of master equations describing the system can became too large for real multilevel atoms (like Cs or Rb) and, therefore, such analysis can require relevant computer resources. By contrast, the quantum trajectories analysis of the multilevel atomic system with large number N of energy levels requires computational resources proportional to N and, therefore, has an advantage here. Despite this difference, each of the two techniques has its own advantages and drawbacks, so that we intentionally consider both of them to clarify which one is better and in which situation.

2.1. Density matrix analysis

We will start with the density matrix analysis, when the dynamics of a quantum system is described with the density matrix time dependence of which is defined by the following kinetic or *master equation*:

$$\dot{\hat{\rho}} = -\frac{i}{\hbar}[\hat{H}, \hat{\rho}] + \mathcal{L}_{\text{relax}}\hat{\rho}, \tag{1}$$

where first term in the right part of the equation describes reversible dynamics of the system with the hamiltonian $\hat{H}$ and second term—nonreversible dynamics of the system due to the stochastic interaction of the system with the reservoir, which is described with the relaxation superoperator $\mathcal{L}_{\text{relax}}$. In assumption that interaction of the system with the reservoir can be described with a diffusion type process, the relaxation superoperator can be presented as the averaged over the reservoir noise $\hat{\xi}$ of the secondary commutator with the hamiltonian $\hat{H}_\xi$ of the system–reservoir interaction.

Then, the relaxation term $\mathcal{L}_{\text{relax}}\rho$ in master equation (1) can be written in the general Lindblad form [17] as

$$\mathcal{L}_{\text{relax}} = -\frac{1}{2}\sum_m (\hat{C}_m^\dagger \hat{C}_m \odot + \odot \hat{C}_m^\dagger \hat{C}_m) + \sum_m \hat{C}_m \odot \hat{C}_m^\dagger, \tag{2}$$

where $\odot$ is the substitution symbol to be replaced with the density matrix $\hat{\rho}$, operators $\hat{C}_m$ describe interaction with the reservoir, operators $\hat{C}_m^\dagger$ are conjugated to the operators $\hat{C}_m$ and both of them have dimension $(1/t)^{1/2}$.

It is worth to note that representation (2) preserves interpretation of $\hat{\rho}$ as the density matrix, i.e., we should fulfill the condition $\text{Tr}\hat{\rho} = 1$ and the probability $\langle\psi|\,\hat{\rho}\,|\psi\rangle$ of finding the system in any state $|\psi\rangle$ must be positive or equal to zero at any time moment and for any $\hat{\rho}(t=0)$. Note also that Eq. (2) does not require that $\hat{C}_m$ must be defined uniquely.

In Eq. (2) the first sum is the anti-commutator, which consists of the terms decreasing the total population $\text{Tr}\hat{\rho}$; the second sum contributes to $(d/dt)\text{Tr}\hat{\rho}$. The number of operators $\hat{C}_m$ in Eq. (2) in general case can be rather large because each operator corresponds to a specific decay channel. For the case of spontaneous emission in a two-level system, for instance, there exists only one operator because we consider only one decay channel, i.e., spontaneous decay. This operator has the form $\hat{C}_1 = \Gamma^{1/2}\hat{\sigma}^-$, where $\hat{\sigma}^- = |g\rangle\langle e|$ is the atomic transition operator from the ground state $|g\rangle$ onto the excited state $|e\rangle$. More examples are described in Ref. 16.

For the case of a Λ-system, in order to write the operators $\hat{C}_m$ one has to take into account the following relaxation processes: spontaneous decay from the excited state $|3\rangle$, incoherent decay and incoherent pumping of the two ground levels $|1\rangle$, $|2\rangle$. Operator $\hat{C}_m$ in this case will consist of four terms responsible for the above listed relaxation processes, namely, operators $\hat{C}_1$ and $\hat{C}_2$ describe spontaneous decay from the excited state $|3\rangle$ onto the ground states $|1\rangle$, $|2\rangle$, operators $\hat{C}_3$ and $\hat{C}_4$ describe incoherent decay and incoherent pumping of the level $|1\rangle$ to the level $|2\rangle$:

$$\begin{array}{ll} \hat{C}_1 = (\gamma_{31})^{1/2}\hat{P}_{13}, C_1^\dagger = (\gamma_{31})^{1/2}\hat{P}_{31}; & \hat{C}_2 = (\gamma_{32})^{1/2}\hat{P}_{23}, C_2^\dagger = (\gamma_{32})^{1/2}\hat{P}_{32}; \\ \hat{C}_3 = (\gamma_{21})^{1/2}\hat{P}_{12}, C_3^\dagger = (\gamma_{21})^{1/2}\hat{P}_{21}; & \hat{C}_4 = (\mu_{12})^{1/2}\hat{P}_{21}, C_4^\dagger = (\mu_{12})^{1/2}\hat{P}_{12}, \end{array} \tag{3}$$

where $\hat{P}_{kl}$ are the transition operators, which are represented, in general case, by the matrices with the only non-zero kl-element $\hat{P}_{kl}(k,l) = 1$.

With the help of Eqs. (2), (3) the relaxation term $\mathcal{L}_{\text{relax}}\hat{\rho}$ in master equation (1) takes the form:

$$\begin{pmatrix} -\mu_{12}\rho_{11}(t) + \gamma_{21}\rho_{22}(t) + \gamma_{31}\rho_{33}(t) & -0.5(\gamma_{21}+\mu_{12})\rho_{12}(t) & -0.5(\gamma_{31}+\gamma_{32}+\mu_{12})\rho_{13}(t) \\ -0.5(\gamma_{21}+\mu_{12})\rho_{12}(t) & \mu_{12}\rho_{11}(t) - \gamma_{21}\rho_{22}(t) + \gamma_{32}\rho_{33}(t) & -0.5(\gamma_{31}+\gamma_{32}+\gamma_{21})\rho_{23}(t) \\ -0.5(\gamma_{31}+\gamma_{32}+\mu_{12})\rho_{13}(t) & -0.5(\gamma_{31}+\gamma_{32}+\gamma_{21})\rho_{23}(t) & -(\gamma_{31}+\gamma_{32})\rho_{33}(t), \end{pmatrix} \quad (4)$$

where γ_{31}, γ_{32} are the spontaneous decay rates, γ_{12} and μ_{12} are the decay and pumping rates of the level $|1\rangle$ via the level $|2\rangle$, respectively.

Now, master equation (1) can be integrated numerically for a given Hamiltonian $\hat{H}$ of the system and then all its necessary characteristics can be modeled.

2.2. Quantum trajectories analysis

Another relevant approach to model the temporal behavior of a Λ-system is the quantum trajectories analysis [13–16], which uses instead of the time-dependent density matrix statistically-equivalent stochastic temporal dynamics of the wave function with the following averaging of the results by analogy with the Monte-Carlo method.

Modeling evolution of the wave function on the discretization interval dt, which ensures identical results with the solution of the master equation (1), includes two parts: i) modeling continuous variation of the current state and ii) modeling quantum jumps occurring randomly with certain probability.

Let us assume that the system at time t is in the state $|\psi(t)\rangle$. Then, the continuous variation of the current state can be described with the temporal dynamics of the wave function $\left|\psi^{(1)}(t)\right\rangle$, which is governed by the Schrödinger equation

$$\left|\psi^{(1)}(t+\delta t)\right\rangle \approx (1 + \frac{1}{i\hbar}\hat{\tilde{H}}dt)\,|\psi(t)\rangle \quad (5)$$

with the non-hermitian hamiltonian

$$\hat{\tilde{H}} = \hat{H} - \frac{i\hbar}{2}\sum_m \hat{C}_m^\dagger \hat{C}_m. \quad (6)$$

New wave-function is not normalized because the hamiltonian $\tilde{H}$ is a non-hermitian one and the squared norm of the function is equal to $\left\langle\psi^{(1)}(t+dt)\right|\,|\psi(t+dt)\rangle = 1 - \delta p$, where δp has the form:

$$\delta p = \sum_m \delta p_m = dt \sum_m \langle\psi(t)|\,\hat{C}_m^\dagger \hat{C}_m\,|\psi(t)\rangle, \quad (7)$$

where the time step dt must fulfill the inequality $\delta p \ll 1$.

Random behavior of the wave function is described with the probability δp of quantum jumps. If the quantum jump does not occur with the probability $1 - \delta p$, the wave function $\left|\psi^{(1)}(t+\delta t)\right\rangle$ must be renormalized to unit and then it will be mapped with the corresponding normalized function $|\psi(t+\delta t)\rangle$. When the quantum jump occurs, the wave-function transfers into the state $C_m\,|\psi(t)\rangle$ with the related probability $\delta p_m/\delta p$. Thus, at the time moment $t + \delta t$ we do have one of the two normalized wave-functions:

- with the probability $1 - \delta p$ the quantum jump does not occur and $|\psi(t+\delta t)\rangle = \left|\psi^{(1)}(t+\delta t)\right\rangle(1-\delta p)^{-1/2}$,
- with the probability δp_m the quantum jump occurs and $|\psi(t+\delta t)\rangle = \hat{C}_m\,|\psi(t)\rangle(\delta p_m/\delta t)^{-1/2}$.

3. WHICH PHYSICAL QUANTITIES ARE OF INTEREST TO CALCULATE?

Physical quantities that are of interest and can be measured experimentally include the total fluorescence intensity in equilibrium and in the transient response, resonance fluorescence spectrum, linear and nonlinear absorption coefficients, and the refractive indices.

3.1. Spontaneous fluorescence intensity

The spontaneous fluorescence intensity is proportional to the excited-state population,

$$I_{\text{fl}} \sim \hat{n}_3 = \langle 3|\,|3\rangle\,. \tag{8}$$

and its total intensity is proportional to the stationary value of the excited-state population:

$$I_{\text{fl}}^{\text{total}} \sim \langle \hat{n}_3 \rangle = \langle\langle 3|\,|3\rangle\rangle. \tag{9}$$

It is worth to note here that a typical experiment spectroscopy of coherent dark resonances is carried out in a vapor cell. Therefore, every atom is spending a finite amount of time τ_t interacting with the laser radiation before it is depolarized for instance by wall collisions. Important is that an atom has a transient response to the laser fields, or more precisely the time τ_p it takes for an atom to reach the coherent dark state by optical pumping. Let us assume that initially atom is in an incoherent superposition of levels $|1\rangle$ and $|2\rangle$. Then, due to the field action onto the coupled state, it goes to the excited state. Finally, it reaches the uncoupled state due to the decay of the excited state, so that we find the excited state being significantly depopulated. Obviously the time τ_p, which depends on the relaxation parameters, should be at least much shorter than the longest observation time τ_t that can be achieved in the experiment. Within the Markov approach the inverse time distribution has a Lorentzian shape.

3.2. Resonance fluorescence spectrum

The spectrum of resonance fluorescence of a driven Λ-system is typically derived from the correlation function of the frequency-positive and frequency-negative operators of the complex amplitudes $\hat{\sigma}_{13}^{\pm}$, $\hat{\sigma}_{23}^{\pm}$ [18] related to the corresponding Pauli matrices $\hat{\sigma}_{13}^{\mp}, \hat{\sigma}_{23}^{\mp}$ that are the transition operators $|k\rangle\langle l|$ with $k \neq l = 1,2$. Respective theoretical calculations have been made both in rotating wave approximation (RWA) and beyond it in Refs. 19,20.

3.3. Absorption

Absorption of the laser light transmitted through a vapor cell is characterized by the absorption coefficient α causing the reduction of an electromagnetic wave with intensity $I = c\epsilon_0 E\,E^*/2$ [20]:

$$\alpha = \frac{1}{I(z)}\frac{dI(z)}{dz} = \frac{\omega}{2I(z)}\Im\text{m}(\langle\hat{P}\rangle E^*), \tag{10}$$

where $\omega \approx \omega_{L1}, \omega_{L2}$. The polarizations $\hat{P}_{13}(\omega_{L1})$, $\hat{P}_{23}(\omega_{L2})$ acting on laser fields with frequencies and amplitudes $\hat{E}_{L1}$, ω_{L1} and $\hat{E}_{L2}$, ω_{L2} are given by

$$\hat{P}_{13}(\omega_{L1}) = N_0 d_{13}\,|1\rangle\langle 3|, \quad \hat{P}_{23}(\omega_{L2}) = N_0 d_{23}\,|2\rangle\langle 3|, \tag{11}$$

where N_0 is the number of atoms per unit volume. Making use of Eq. (10,11) together with $d_{13}E(\omega_{L1}) = 2\hbar\Omega_{13}$ and $d_{23}E(\omega_{L2}) = 2\hbar\Omega_{23}$ we find that

$$\alpha(\omega_{L1}) = \left(\frac{\hbar\omega\Omega_{13}N_0}{I_{L1}(z)}\right)\Im\text{m}\langle|1\rangle\langle 3|\rangle, \quad \alpha(\omega_{L2}) = \left(\frac{\hbar\omega\Omega_{23}N_0}{I_{L2}(z)}\right)\Im\text{m}\langle|2\rangle\langle 3|\rangle. \tag{12}$$

3.4. Refractive indices

Real part of the refraction index $n = n' + in''$ can be calculated by analogy with the absorption coefficient from

$$n' - 1 = \frac{1}{k}\frac{d\Phi(z)}{dz} = \frac{c}{2I(z)}\Re\text{e}(\langle\hat{P}\rangle\hat{E}^*), \tag{13}$$

where k is the wavevector, yielding

$$n'(\omega_{L1}) - 1 = \left(\frac{\hbar c\Omega_{12}N_0}{I_{L1}(z)}\right)\Re\text{e}\langle|1\rangle\langle 3|\rangle, \quad n'(\omega_{L2}) - 1 = \left(\frac{\hbar c\Omega_{23}N_0}{I_{L2}(z)}\right)\Re\text{e}\langle|2\rangle\langle 3|\rangle. \tag{14}$$

The dispersion coefficients are nonlinear ones since the density matrix elements depend on both laser light fields, I_{L1}, I_{L2}.

4. MODELING FLUORESCENCE FROM A DRIVEN Λ-SYSTEM

4.1. Case when the frequency modulation is switched off

Before studying interaction of a Λ-system with the frequency-modulated laser field, let us first analyze a more simple problem—how the Λ-system interacts with a resonant laser field without frequency modulation.

4.1.1. Density matrix analysis

Let us consider a three-level quantum system in Λ-configuration, which interacts with the field $E(t) = E_0 \cos(\omega_0 t + \varphi)$. The interaction hamiltonian has the form:

$$\hat{H} = \frac{\hbar}{2} \begin{pmatrix} 0 & 0 & \Omega_{13} \\ 0 & -\omega_{12} & \Omega_{23} \\ \Omega_{13} & \Omega_{23} & \delta_L, \end{pmatrix} \tag{15}$$

where Ω_{13}, Ω_{23} are the Rabi frequencies, $\delta_L = \omega_0 - \omega_{13}$ is the one-photon frequency detuning of the probe laser field from the resonance, ω_{12} is the frequency shift between two ground levels (see Fig. 1).

Substituting the relaxation operator (2) in Eq. (1) we receive the following set of differential equations for all density matrix elements:

$$\begin{aligned}
\rho'_{11}(t) &= -\mu_{12}\rho_{11}(t) + \gamma_{21}\rho_{22}(t) + i(\Omega_{13}\rho_{13}(t) - \Omega_{13}\rho_{31}(t)) + \gamma_{31}\rho_{33}(t), \\
\rho'_{12}(t) &= -\Gamma_{12}\rho_{12}(t) - i(\omega_{12}\rho_{12}(t) + \Omega_{23}\rho_{13}(t) - \Omega_{13}\rho_{32}(t)), \\
\rho'_{13}(t) &= -\Gamma_{13}\rho_{13}(t) + i(\Omega_{13}\rho_{11}(t) + \Omega_{23}\rho_{12}(t) + \delta_L\rho_{13}(t) - \Omega_{13}\rho_{33}(t)), \\
\rho'_{21}(t) &= -\Gamma_{21}\rho_{21}(t) + i(\omega_{12}\rho_{21}(t) + \Omega_{13}\rho_{23}(t) - \Omega_{23}\rho_{31}(t)), \\
\rho'_{22}(t) &= \mu_{12}\rho_{11}(t) - \gamma_{21}\rho_{22}(t) + i(\Omega_{23}\rho_{23}(t) - \Omega_{23}\rho_{32}(t)) + \gamma_{32}\rho_{33}(t), \\
\rho'_{23}(t) &= -\Gamma_{32}\rho_{23}(t) + i(\Omega_{13}\rho_{21}(t) + \Omega_{23}\rho_{22}(t) + \omega_{12}\rho_{23}(t) + \delta_L\rho_{23}(t) - \Omega_{23}\rho_{33}(t)), \\
\rho'_{31}(t) &= -\Gamma_{31}\rho_{31}(t) + i(-\Omega_{13}\rho_{11}(t) - \Omega_{23}\rho_{21}(t) - \delta_L\rho_{31}(t) + \Omega_{13}\rho_{33}(t)), \\
\rho'_{32}(t) &= -\Gamma_{32}\rho_{32}(t) + i(-\Omega_{13}\rho_{12}(t) - \Omega_{23}\rho_{22}(t) - (\omega_{12} + \delta_L)\rho_{32}(t) + \Omega_{23}\rho_{33}(t)), \\
\rho'_{33}(t) &= i(-\Omega_{13}\rho_{13}(t) - \Omega_{23}\rho_{23}(t) + \Omega_{13}\rho_{31}(t) + \Omega_{23}\rho_{32}(t)) - (\gamma_{31} + \gamma_{32})\rho_{33}(t).
\end{aligned} \tag{16}$$

Integrating this set of differential equations we obtain a complete picture of temporal dynamics of the driven Λ-system and can calculate any its characteristic. If we are interested in the fluorescence, which is proportional to the excited state population, one needs simply to calculate the population of the excited state $|3\rangle$ (see Eq. refIspfl-trans. This temporal dependency is shown in Fig. 2a versus the frequency splitting ω_{12} between two ground levels.

From Fig. 2 one can see that for the case when only one laser field with the frequency ω_L acts on both transitions $|1\rangle \leftrightarrow |2\rangle$ and $|2\rangle \leftrightarrow |3\rangle$ of the Λ-system, the dark resonance is observed at $\omega_{12} = \omega_L - \omega_L = 0$, i.e., for the case of degenerate Λ-system. In experiment, such situation corresponds to the case when no external magnetic field is applied to the quantum system.

4.1.2. Quantum trajectories analysis

For simplicity, we will consider only two radiation decays in the Λ-system from excited state $|3\rangle$ onto the low-lying states $|1\rangle$, $|2\rangle$, reducing the number of operators $\hat{C}_m$ in Eq. (2) just to two operators: $\hat{C}_1 = (\gamma_{31})^{1/2}\hat{\mathrm{P}}_{13}$ and $\hat{C}_2 = (\gamma_{32})^{1/2}\hat{\mathrm{P}}_{23}$.

Inserting $\hat{C}_1$ and $\hat{C}_2$ into Eq. (2), we obtain equation for the relaxation part $\mathcal{L}_{\mathrm{relax}}\hat{\rho}$:

$$\begin{pmatrix} \gamma_{31}\rho_{33}(t) & 0 & -0.5(\gamma_{31} + \gamma_{32})\rho_{13}(t) \\ 0 & \gamma_{32}\rho_{33}(t) & -0.5(\gamma_{31} + \gamma_{32})\rho_{23}(t) \\ -0.5(\gamma_{31} + \gamma_{32})\rho_{13}(t) & -0.5(\gamma_{31} + \gamma_{32})\rho_{23}(t) & -(\gamma_{31} + \gamma_{32})\rho_{33}(t). \end{pmatrix}. \tag{17}$$

In accordance with the results of Sec. 2.2, the non-hermitian interaction hamiltonian is given by Eq. (6). Substituting $\hat{C}_1$ and $\hat{C}_2$ in this equation leads to the hamiltonian of the form:

$$\hat{H} = \frac{\hbar}{2} \begin{pmatrix} 0 & 0 & \Omega_{13} \\ 0 & -\omega_{12} & \Omega_{23} \\ \Omega_{13} & \Omega_{23} & -i\Gamma + \delta_L \end{pmatrix}, \tag{18}$$

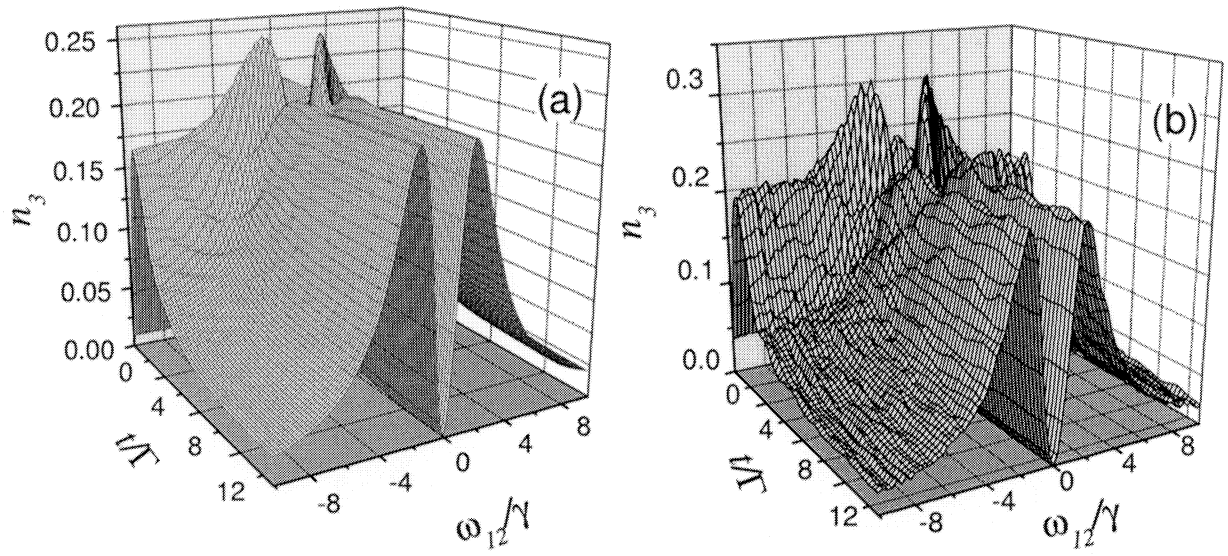

Figure 2. Temporal dependence of the excited state population from a driven Λ-system calculated with the help of density matrix approach (a) and using quantum trajectories technique (b). Both plots show similar dependence of the excited state population n_3 versus time since the excitation of the system and the ground state frequency splitting ω_{12}. For simplicity, the calculations were made for the case of a symmetric Λ-system, i.e., for the equal Rabi frequencies $\Omega_{13} = \Omega_{23} = 1$ and equal spontaneous decay rates $\gamma_{31} = \gamma_{32} = \gamma = 1$ from the excited state; relaxation parameters of the ground state were set to zero. The number of computed quantum trajectories for figure (b) is equal to 2000.

where $\Gamma = (\gamma_{31} + \gamma_{32})/2$.

From Schrödinger equation (5) one can readily obtain the following set of differential equations for the probability amplitudes $a_1(t)$, $a_2(t)$, and $a_3(t)$:

$$\begin{aligned} a_1'(t) &= -i\Omega_{13}a_3(t) \\ a_2'(t) &= -i(-\omega_{12}a_2(t) + \Omega_{23}a_3(t)) \\ a_3'(t) &= -i(\Omega_{13}a_3(t) + \Omega_{23}a_2(t) + (-i\Gamma + \delta_L)a_3(t)). \end{aligned} \tag{19}$$

Let us assume then that initially, at $t = 0$, all population in the system was equally distributed among the states $|1\rangle$ and $|2\rangle$, i.e., $n_1 = n_2 = 0.5$. Then, the set of equations (19) can be integrated using the quantum trajectories technique, which leads to the time-dependent wave-functions and, respectively, to the temporal dependencies of the population of the system's levels.

Temporal dependency of the excited state population calculated with the help of quantum trajectories technique is shown in Fig. 2b versus the frequency detuning ω_{12} of the two ground states. From Fig. 2b one can clearly see that the stationary solution is reached at the time of the order of $10\gamma_{31}$.

A more detailed comparison of the simulation results obtained by the density matrix approach and with quantum trajectories technique is shown in Fig. 3. It clearly shows that both methods give similar results and the curves are coincide rather well.

4.2. Case when the frequency modulation is switched on

In this Section, we will analyze the spectrum of the Λ-system driven by a resonant frequency-modulated laser field $E(t)$ with the carrier frequency ω_0, which for the case of harmonic modulation with the modulation index M and frequency modulation Ω can be written as

$$E(t) = E_0 \exp[i(\omega_0 t + M \sin \Omega t)] = E_0 \exp(i\omega_0 t) \sum_{n=-\infty}^{+\infty} J_n(M) \exp(in\Omega t). \tag{20}$$

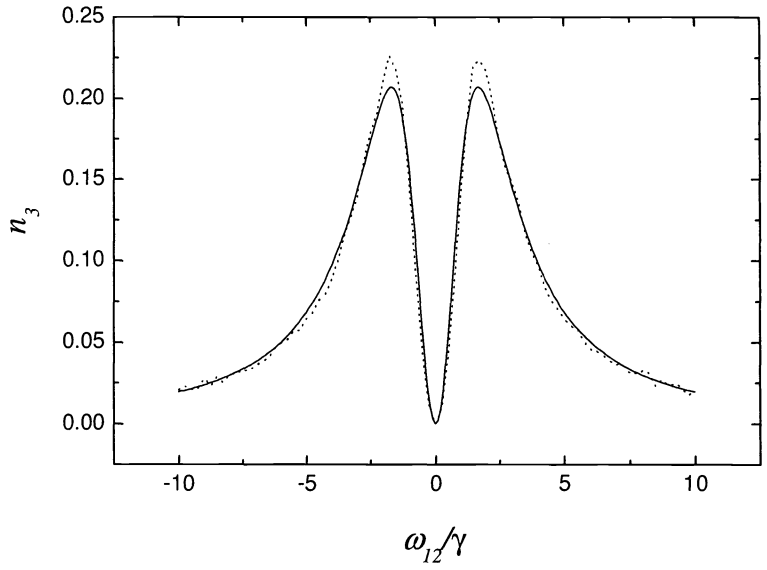

Figure 3. Calculated population of the excited state of the symmetric Λ-system ($\gamma_{31} = \gamma_{32} = \gamma$, $\Gamma = 1$) versus ω_{12} for $\Omega_{13} = \Omega_{23} = 1$ received with the help of density matrix approach (solid line) and quantum trajectories techniques (dotted line, the number of computed trajectories is equal to 2000) at $t/\Gamma = 14$, i.e., in the steady-state case.

In this series expansion, the Bessel functions $J_n(M)$ characterize the frequency components of the frequency-modulated light, i.e., the amplitudes of the respective spectrum components are proportional to the Bessel functions for the fixed modulation index M. The modulation index is equal to the ratio of the deviation frequency D to the modulation frequency Ω: $M = D/\Omega$. Fig. 4 illustrates how the variation in the modulation index M and the modulation frequency Ω affect the spectrum of the Λ-system. One can see from this figure that at the fixed Ω increasing the deviation frequency leads to the increase of the modulation index and, as a result, to the increase in the number of spectrum lines, which are equidistantly distributed in the spectrum. At the fixed deviation frequency, decreasing the modulation frequency leads to the increase of M and, respectively, the frequency separation between spectral lines decreases.

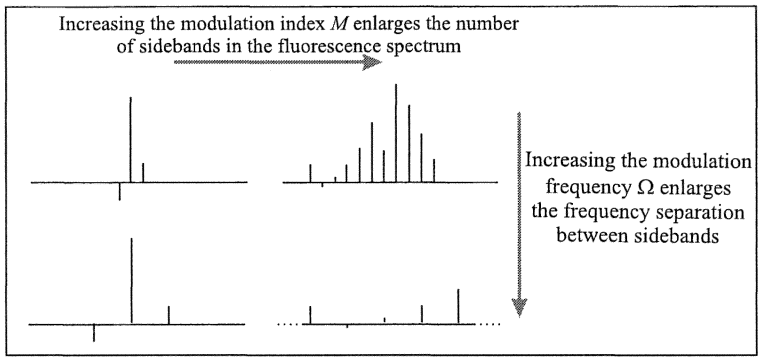

Figure 4. Modification of the fluorescence spectrum of the Λ-system excited by the frequency-modulated laser field due to the variations in the modulation frequency Ω and the modulation index M.

4.2.1. Density matrix analysis

The interaction hamiltonian of the Λ-system interacting with the frequency-modulated laser field $E(t) = E_0 \exp[i(\omega_0 t + M\cos\Omega t)]$ has the form:

$$\hat{H} = \begin{pmatrix} 0 & 0 & e^{i\Delta(t)}\Omega_{13} \\ 0 & -\omega_{12} & e^{i\Delta(t)}\Omega_{23} \\ e^{-i\Delta(t)}\Omega_{13} & e^{-i\Delta(t)}\Omega_{23} & \delta_L, \end{pmatrix} \tag{21}$$

where $\Delta(t) = M\sin\Omega t$. Inserting equation for $\mathcal{L}_{\text{relax}}(\rho_S)$ in the form (4) into Eq. (1), we obtain the following set of differential equations:

$$\begin{aligned}
\rho'_{11}(t) &= -\mu_{12}\rho_{11}(t) + \gamma_{21}\rho_{22}(t) + i(e^{-i\Delta(t)}\Omega_{13}\rho_{13}(t) - e^{i\Delta(t)}\Omega_{13}\rho_{31}(t)) + \gamma_{31}\rho_{33}(t), \\
\rho'_{12}(t) &= -\Gamma_{12}\rho_{12}(t) + i(-\omega_{12}\rho_{12}(t) + e^{-i\Delta(t)}\Omega_{23}\rho_{13}(t) - e^{-i\Delta(t)}\Omega_{13}\rho_{32}(t)), \\
\rho'_{13}(t) &= -\Gamma_{13}\rho_{13}(t) + i(e^{i\Delta(t)}\Omega_{13}\rho_{11}(t) + e^{i\Delta(t)}\Omega_{23}\rho_{12}(t) + \delta_L\rho_{13}(t) - e^{i\Delta(t)}\Omega_{13}\rho_{33}(t)), \\
\rho'_{21}(t) &= -\Gamma_{21}\rho_{21}(t) + i(\omega_{12}\rho_{21}(t) + e^{-i\Delta(t)}\Omega_{13}\rho_{23}(t) - e^{i\Delta(t)}\Omega_{23}\rho_{31}(t)), \\
\rho'_{22}(t) &= \mu_{12}\rho_{11}(t) - \gamma_{21}\rho_{22}(t) + i(e^{-i\Delta(t)}\Omega_{23}\rho_{23}(t) - e^{i\Delta(t)}\Omega_{23}\rho_{32}(t)) + \gamma_{32}\rho_{33}(t), \\
\rho'_{23}(t) &= -\Gamma_{23}\rho_{23}(t) + i(\Omega_{13}\rho_{21}(t) + e^{i\Delta(t)}\Omega_{23}\rho_{22}(t) + \delta_L\rho_{23}(t) + \omega_{12}\rho_{23}(t) + e^{i\Delta(t)}\Omega_{23}\rho_{33}(t)), \\
\rho'_{31}(t) &= -\Gamma_{31}\rho_{31}(t) + i(-e^{-i\Delta(t)}\Omega_{13}\rho_{11}(t) - e^{-i\Delta(t)}\Omega_{23}\rho_{21}(t) - \delta_L\rho_{31}(t) + e^{-i\Delta(t)}\Omega_{13}\rho_{33}(t)), \\
\rho'_{32}(t) &= -\Gamma_{32}\rho_{32}(t) + i(-e^{-i\Delta(t)}\Omega_{13}\rho_{12}(t) - e^{-i\Delta(t)}\Omega_{23}\rho_{22}(t) - \delta_L\rho_{32}(t) - \omega_{12}\rho_{32}(t) + e^{-i\Delta(t)}\Omega_{23}\rho_{33}(t)), \\
\rho'_{33}(t) &= i(-e^{-i\Delta(t)}\Omega_{13}\rho_{13}(t) - e^{-i\Delta(t)}\Omega_{23}\rho_{23}(t) + e^{i\Delta(t)}\Omega_{13}\rho_{31}(t) + e^{i\Delta(t)}\Omega_{23}\rho_{32}(t)) - (\gamma_{31} + \gamma_{32})\rho_{33}(t).
\end{aligned} \tag{22}$$

Solving this set of equations by analogy with Sec. 4.1.1, one can calculate the temporal dependence of the populations of the Λ-system levels.

The temporal dynamics of forming the spectrum of the dark resonance at the fixed modulation frequency and for two values of the modulation index is shown in Fig. 5. Simple analysis of this dynamics shows that with increasing the modulation index the structure of the spectrum is enriched and the number of sideband resonances is increased, too.

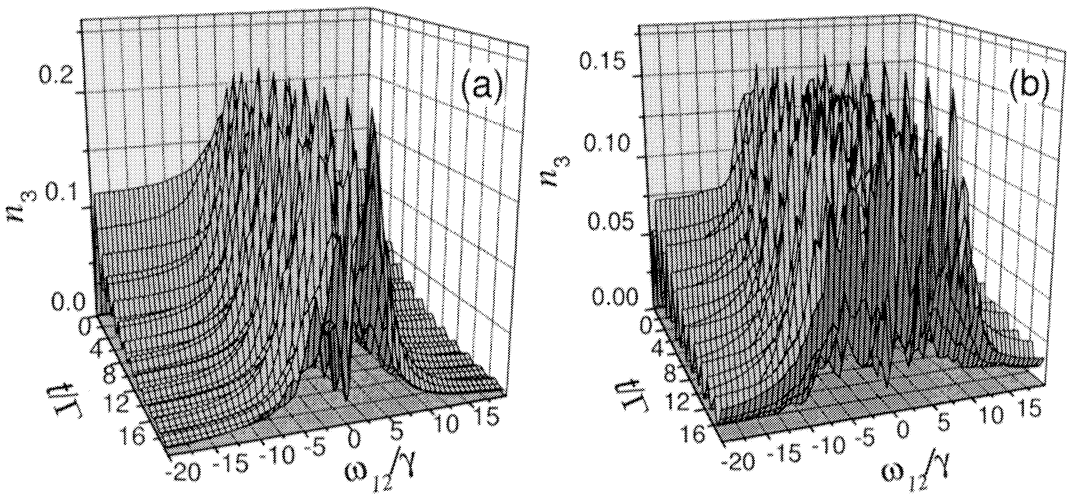

Figure 5. Excited state population of the Λ-system versus time since the excitation of the system and ω_{12} at the fixed modulation frequency $\Omega = 2$ for two values of the modulation index $M = 1.5$ (a) and $M = 4$ (b). Other parameters were chosen as follows: $\Omega = 2$, $\Omega_{13} = \Omega_{23} = 0.8$, $\gamma_{31} = \gamma_{32} = 1$.

Qualitatively, the mechanism of forming the additional dark resonances in the spectrum of a Λ-system under the action of a frequency-modulated laser field is clarified in Fig. 6. Every time a narrow dark resonance is formed when the frequency splitting ω_{12} between two ground levels of the Λ-system exactly matches the frequency difference between two neighboring sidebands in the spectrum of the incident frequency-modulated

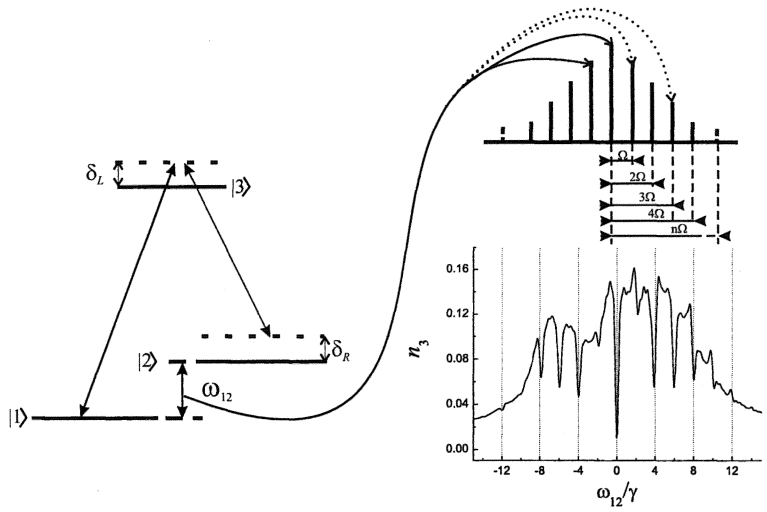

Figure 6. Mechanism of forming the dark resonances for the case of the Λ-system interacting with the frequency-modulated laser field.

laser field. All pairs of the components of the incident laser field spectrum with the frequency shift between them equal to the modulation frequency Ω (for instance, the pair marked by the solid line with arrows in Fig. 6) contribute to the dark resonance for which $\omega_{12} = \Omega$. Also, all the pairs of the components of the incident laser field spectrum frequency shift between which is equal to the doubled modulation frequency 2Ω (for example, the pair marked with the dashed lines with arrows in Fig. 6) contribute to the dark resonance for which $\omega_{12} = 2\Omega$ and so on. From this consideration it follows that the frequency shift between the neighboring resonances in the observed spectrum of the Λ-system is equal to the modulation frequency Ω.

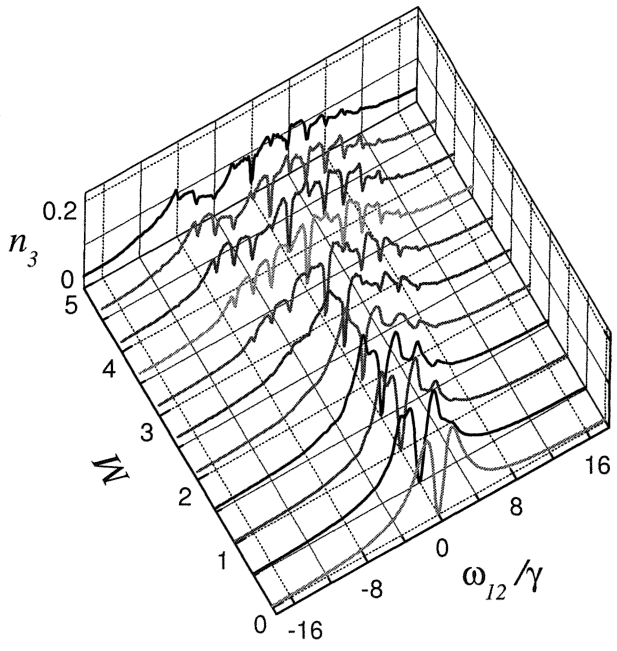

Figure 7. Excited state population versus ω_{12} and the modulation index M. Other parameters were chosen as follows: $\Omega = 2$, $\Omega_{13} = \Omega_{23} = 0.8$, $\gamma_{31} = \gamma_{32} = \gamma = 1$.

The resulting rather complicated spectrum of the Λ-system irradiated with the frequency-modulated resonant laser field is shown in Fig. 7, which plots the population of the excited state of the Λ-system versus the ω_{12} frequency at the fixed modulation frequency $\Omega = 2$ for various values of the modulation index. At $M = 0$, we have no modulation at all and the dark resonance is observed at $\omega_{12} = 0$, i.e., we have the case of degenerated Λ-system. Increasing further the modulation index leads to appearing of additional resonances in the spectrum at the conditions $\omega_{12} = n\Omega$, $n = \pm 1, \pm 2, \pm 3, \ldots$. This is because the number of sidebands in the spectrum of the incident laser field increases with increasing the modulation index in accordance with Eq. (20).

Amplitudes of these sidebands in the spectrum of the incident frequency-modulated laser field are proportional to the Bessel functions $J_n(M)$ at the fixed value of the modulation index M and decreasing up to zero with increasing n. Therefore, the number of sidebands in the spectrum of the incident laser field in the central part of the spectrum is approximately equal to M. Respectively, the resulting spectrum of the Λ-system shows also approximately M dark resonances in the central part of the spectrum. Fig. 8 confirms this result.

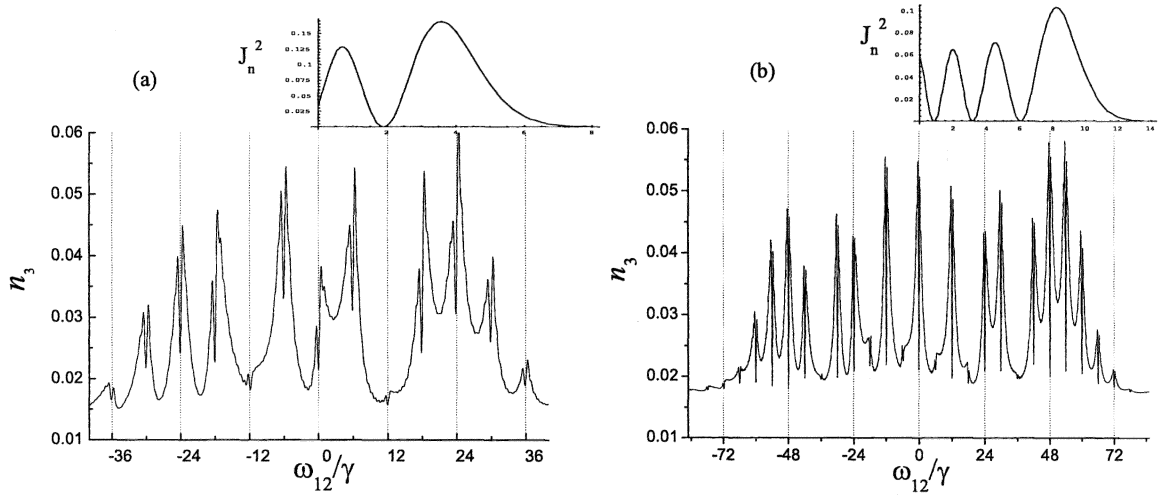

Figure 8. Population of the excited state in the symmetric Λ-system versus ω_{12} for two fixed values of the modulation index $M = 5$ (a) and $M = 10$ (b) at the modulation frequency $\Omega = 6$ a.u. and the Rabi frequencies $\Omega_3 = \Omega_{23} = 0.8$. Insets show the respected squared Bessel functions $J_n^2(M)$.

One can clearly see that at $M = 5$ (Fig. 8a) the resonance at the frequency $\omega_{12} = \pm 2\Omega$ is practically vanishes. At $M = 10$ (Fig. 8b), the resonances at the frequencies $\omega_{12} = \pm\Omega, \pm 3\Omega$ and $\pm 6\Omega$ are vanished, as well. This happens because the two-photon dark resonances are observed on the background of the one-photon ones. As it has been shown in Ref. 21, for example, the power of the modulated signal transmitted through the media is proportional to the squared Bessel function $J_n^2(M)$ for the given M. Keeping in mind that the Bessel function takes zero values at $n = \pm 2$ for $M = 5$ and at $n = \pm 1, \pm 3, \pm 6$ for $M = 10$, this clarifies why the resonances at the frequencies $n\Omega$ for these values of n are practically vanished.

4.2.2. Quantum trajectories analysis

The non-hermitian interaction hamiltonian of the Λ-system interacting with the frequency-modulated laser field $E(t) = E_0 \exp[i(\omega_0 t + M \cos \Omega t)]$ has the form:

$$\hat{\tilde{H}} = \begin{pmatrix} 0 & 0 & e^{i\Delta(t)}\Omega_{13} \\ 0 & -\omega_{12} & e^{i\Delta(t)}\Omega_{23} \\ e^{-i\Delta(t)}\Omega_{13} & e^{-i\Delta(t)}\Omega_{23} & \delta_L - i\Gamma, \end{pmatrix} \tag{23}$$

where $\Delta(t) = M \sin \Omega t$, $\Gamma = (\gamma_{31} + \gamma_{32})/2$.

From Schrödinger equation (5) one can readily obtain the following set of differential equations for the probability amplitudes $a_1(t)$, $a_2(t)$, and $a_3(t)$:

$$\begin{aligned} a_1'(t) &= -ie^{i\Delta(t)}\Omega_{13}a_3(t) \\ a_2'(t) &= -i(-\omega_{12}a_2(t) + e^{i\Delta(t)}\Omega_{23}a_3(t)) \\ a_3'(t) &= -i(e^{i\Delta(t)}\Omega_{13}a_3(t) + e^{i\Delta(t)}\Omega_{23}a_2(t) + (-i\Gamma + \delta_L)a_3(t)). \end{aligned} \tag{24}$$

Let us assume by analogy with Sec. 4.1.2 that at the initial time moment $t = 0$ all population in the system is distributed in between two ground levels $|1\rangle$ and $|2\rangle$, .i.e., $n_1 = n_2 = 0.5$. Then, solving set of equations (24) with the help of quantum trajectories technique we will receive time-dependent wave-functions of the system and time-dependent populations of each of the energetic levels.

Temporal dependency of the population of the excited state calculated with the help of quantum trajectories versus the frequency spacing between two ground levels ω_{12} is shown in Fig. 9. The calculations were done for the same parameters as similar calculations by density matrix approach (Sec. 4.2.1). Comparison of both these methods is shown in Fig. 9b. One can easily see from this figure that results obtained by two different methods are in good agreement. Some quantitative difference is because the number of calculated trajectories is not an infinitive one, but equal only to 5000. Increasing the number of trajectories in a computer experiment will lead to more precise coincidence of the results, but is timeconsuming. However, even our results show that the quantum trajectories technique can be adequately used for simulating not only three level system in Λ-configuration interacting with the frequency-modulated field, but also can be used for simulating more complicated multilevel systems.

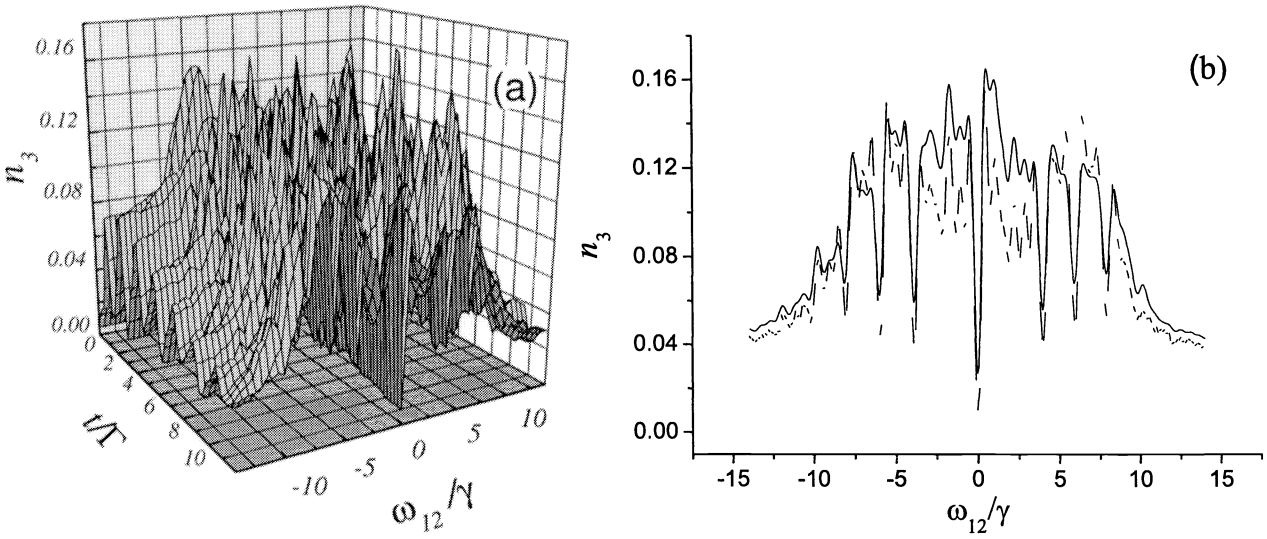

Figure 9. a) Excited state population of the Λ-system versus time since the excitation of the system and ω_{12} at the fixed modulation frequency $\Omega = 2$ for the modulation index $M = 4$. Other parameters were chosen as follows: $\Omega = 2$, $\Omega_{13} = \Omega_{23} = 0.8$, $\Gamma = 1$. b) Excited state population of the Λ-system versus ω_{12} for the parameters of (a) computed with the help of density matrix approach (solid line) and quantum trajectories techniques (dashed line). The number of computed trajectories is equal to 5000.

5. CONCLUSIONS

In conclusions, we have presented a theoretical model for the frequency-modulation spectroscopy of dark resonances on example of a three-level quantum system in Λ-configuration driven by resonant laser field(s) with and without frequency modulation using two simulation techniques—the density matrix and quantum trajectories analysis. With these techniques, such physical quantities as the total fluorescence intensity in equilibrium and

in the transient response, resonance fluorescence spectrum, linear and nonlinear absorption coefficients, and the refractive indices, which can be all measured experimentally, can be modeled within the frame of the proposed model.

As an example, we have calculated the total fluorescence intensity in equilibrium and in the transient response for the real atomic Λ-system formed of the Zeeman sublevels of one of the two alkali hyperfine ground states, specifically in Cs atoms. The calculated spectrum using such a simplified model is in a qualitative agreement with the experimental results reported in the literature [9,10] and it is clearly seen that at high laser modulation index additional side CPT-resonances are present. Their frequency positions matches the experimental ones and it can be seen that CPT resonance appear when Ω/n (where n is an integer number) equals the Zeeman splitting of two sublevels ω_{12}.

Our future work will be concentrated on elaboration of more complex model, where a larger number of experimental parameters will be considered. Moreover, we plan to extend the model by considering a richer level structure, which is well reasonable using the method of quantum trajectories analysis, whose computing time increases linearly with the number N of the considered levels, in contrast with the quadratic dependency shown by the density matrix approach.

ACKNOWLEDGMENTS

This work was partially supported by the Russian Foundation for Basic Research under the grant No. 04–02–17554.

REFERENCES

1. G. Alzetta, A. Gozzini, L. Moi, G. Orriols, Nuovo Cimento. B. **36**, 5 (1976).
2. H. R. Gray, R. M. Whitly, and C. R. Stroud (Jr), Opt. Lett. **3**, 218 (1978).
3. G. Alzetta, L. Moi, G. Orriols, Nuovo Cimento. B. **52**, 209 (1979).
4. G. Alzetta, L. Moi, G. Orriols, Opt. Commun. **42**, 335 (1982).
5. A. Aspect, E. Arimondo, R. Kaiser, N. Vansteenkiste, C. Cohen-Tannoudji, Phys. Rev. Lett. **61**, 826 (1996).
6. A. Kasapi, Phys. Rev. Lett. **77**, 3908 (1997).
7. E. Arimondo, in *Progress in Optics*, edited by E. Wolf (Elsevier, Amsterdam, 1996), Vol. 35, p. 257.
8. Yu. V. Vladimirova, B. A. Grishanin, V. N. Zadkov, N. N. Kolachevskii, A. V. Akimov, N. A. Kisilev, S. I. Kanorskii, J. of Theor. and Exp. Physics **96**, 629 (2003).
9. C. Andreeva, G. Bevilacqua, V. Biancalana, S. Cartaleva, Y. Dancheva, T. Karaulanov, C. Marinelli, E. Mariotti, and L. Moi, Appl. Phys. B **76**, 667 (2003).
10. G. Bevilacqua, V. Biancalana, E. Breschi, Y. Dancheva, C. Marinelli, E. Mariotti, L. Moi, Ch. Andreeva, T. Karaulanov, S. Cartaleva, 13-th Int. School on Quantum Electr.: Laser Physics and Applications, Proc. SPIE Vol.5830, p. 150-158 (2005).
11. E.B.Alexandrov, M.Azuzinsh, D.Budker, D.F.Kimbal, S.M.Rochester, V.V.Yashchuk, arXiv: Physics 0405049 (2004)
12. Yu.Malakyan, S.M.Rochester, D.Budker, D.F.Kimbal, V.V.Yashchuk, Phys. Rev. A69, 013817 (2004)
13. J.Dalibard, Y. Castin, K. Molmer, Phys. Rev. Lett. **68**, 5, (1992).
14. K. Mölmer and Y. Castin, Quantum Semiclass. Opt. **8**, 49 (1996).
15. H. J. Carmichael, Phys. Rev. Lett. **70**, 15, (1993).
16. K. Mölmer, Y. Castin, and J. Dalibard, J. Opt. Soc. Am. B **10**, 524 (1993).
17. G. Lindblad, Commun. Math. Phys. **48**, 119, (1976).
18. R. J. Glauber, in: *Quantum Optics and Electronics*, ed. C. DeWitt, A. Blandin, C. Cohen-Tannouji, N. Y., 1964.
19. B. A. Grishanin, V. N. Zadkov, and D. Meschede, Phys. Rev. A**58**, 4235 (1998).
20. I. V. Bargatin, B. A. Grishanin, Optics and Spectroscopy **87**, 367 (1999).
21. J.M.Supplee at al., Applied Optics, **33**, 27, (1994).